

## Resonantly Interacting Fermions In a Box

Michael McNeil Forbes,<sup>1,2,3</sup> Stefano Gandolfi,<sup>3</sup> and Alexandros Gezerlis<sup>2,3</sup>

<sup>1</sup>*Institute for Nuclear Theory, University of Washington, Seattle, Washington 98195-1560 USA*

<sup>2</sup>*Department of Physics, University of Washington, Seattle, Washington 98195-1560 USA and*

<sup>3</sup>*Theoretical Division, Los Alamos National Laboratory, Los Alamos, New Mexico 87545, USA*

(Dated: October 24, 2018)

We use two fundamental theoretical frameworks to study the finite-size (shell) properties of the unitary gas in a periodic box: 1) an *ab initio* Quantum Monte Carlo (QMC) calculation for boxes containing 4 to 130 particles provides a precise and complete characterization of the finite-size behavior, and 2) a new Density Functional Theory (DFT) fully encapsulates these effects. The DFT predicts vanishing shell structure for systems comprising more than 50 particles, and allows us to extrapolate the QMC results to the thermodynamic limit, providing the tightest bound to date on the ground-state energy of the unitary gas:  $\xi_S \leq 0.383(1)$ . We also apply the new functional to few-particle harmonically trapped systems, comparing with previous calculations.

PACS numbers: 67.85.-d, 71.15.Mb, 31.15.E-, 03.75.Ss, 24.10.Cn, 03.75.Hh, 21.60.-n

THE FERMION MANY-BODY PROBLEM plays a fundamental role in a vast array of physical systems, from dilute gases of cold atoms to nuclear physics in nuclei and neutron stars. The universal character of this problem – each system is governed by a similar microscopic theory – coupled with direct experimental access in cold atoms, has led to an explosion of recent interest (see Refs. [1] for a review). Despite this broad applicability, we are far from fully understanding even the simplest system: the “unitary gas” comprising equal numbers of two fermionic species interacting with a resonant *s*-wave interaction of infinite scattering length  $a_s \rightarrow \infty$ . Lacking any scale beyond the total density  $n_+ = n_a + n_b$ , the unitary gas eschews perturbative expansion and requires experimental measurement or accurate numerical simulation for a quantitative description – the latter is presently more precise. Typical Quantum Monte Carlo (QMC) calculations, however, can access at most a few hundred particles. Density Functional Theory (DFT) provides a complementary approach through which one may extrapolate these results to large systems beyond the reach of direct simulation.

In this Letter, we present the most precise QMC calculations to date of the unitary gas in a periodic box, studying from 4 to 130 particles, thereby providing a benchmark for many-body theories. We use this to calibrate a local DFT, then use this DFT to study the finite-size effects (“shell” effects in nuclear physics) and extrapolate the QMC results to the thermodynamic limit. We provide the most precise bound to date of the universal Bertsch parameter [2]  $\xi_S = \mathcal{E}/\mathcal{E}_{FG} \leq 0.383(1)$ . ( $\mathcal{E}_{FG} = 3/5n_+E_F$  is the energy density of a free Fermi gas with the same total density  $n_+ = k_F^3/(3\pi^2)$ , and  $E_F = \hbar^2k_F^2/(2m)$  is the Fermi energy.) We also explore the finite-size properties of the DFT – a crucial element in the program to calculate properties of finite nuclei with a universal DFT [3]. We find that a local DFT can capture the finite-size effects in

these systems without the need for particle number projection. We limit our discussion to symmetric systems ( $n_a = n_b$ ), leaving odd-even staggering to future work, as the DFT then requires an additional dimensionless parameter to characterize the asymmetry  $n_a \neq n_b$ .

The QMC results presented here are directly applicable to cold <sup>6</sup>Li or <sup>40</sup>K atoms, and constrain dilute neutron matter in neutron stars [4]; likewise, the general DFT approach has myriads of applications throughout cold-atom and nuclear physics (see Ref. [5] for a review). Our calculation of  $\xi_S$  is consistent with previous results, but an order of magnitude more precise. Continuum QMC bounds  $\xi_S \lesssim 0.40 - 0.44$  with an uncertainty no better than the last digit [4, 6–10]. Lattice QMC results range from  $\xi_S \approx 0.3 - 0.4$  [11–13], comparable to analytic results [14]. Experimental groups found qualitative agreement [15], which led to precision measurements: notably with Duke [16] and Paris [17] quoting 0.39(2) and 0.41(1) respectively.

DFT is an in principle exact approach, widely used in nuclear physics [18], and in quantum chemistry to describe normal (i.e., non-superfluid) systems. It has recently been extended to describe the unitary gas [5, 19–21]. We build upon one approach – the Superfluid Local Density Approximation (SLDA) – which was originally constrained by QMC calculations of the continuum state, and then validated with QMC calculations in a harmonic trap [22, 23] (see also Fig. 2). We focus on translationally invariant systems in a periodic box to isolate the finite-size effects from the gradient effects. We find that the inclusion of an anomalous density is crucial: functionals attempting to model the superfluid by adding only gradient or kinetic corrections [19, 21] are unable to even qualitatively characterize the finite-size effects.

Our QMC results are based on a fixed-node Diffusion Monte Carlo approach that projects out the state of lowest energy from the space of all wave functions with

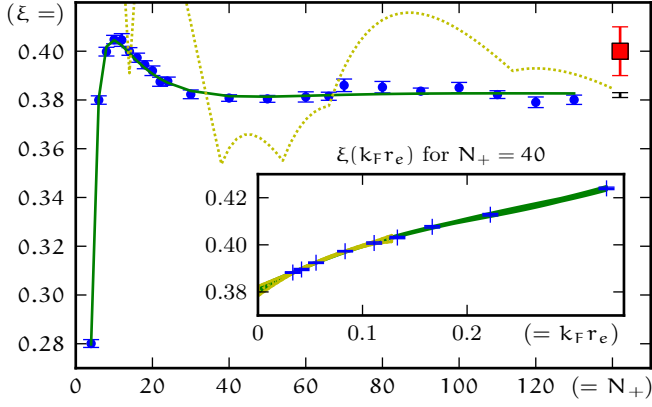


**Figure 1.** (color online) Ground-state energy-density  $\xi = E/E_{\text{FG}}$  of  $N_+$  fermions in a periodic cubic box at the unitary limit. The circles with error bars are the result of using a quadratic least-squares extrapolation to zero effective range of our new QMC results. The solid curve is the best fit SLDA DFT. The light dotted curve is the functional considered in [19] with  $\alpha = 0.69$ . For comparison, we have plotted the previous best estimate  $\xi_S = 0.40(1)$  (red square) and the current estimate  $\xi_S = 0.383(1)$  below it to the far right of the figure. Inset: we show the typical effective-range dependence  $\xi(k_F r_e)$  with the best fit  $1\sigma$  error bounds for all-point cubic (solid dark green) and five-point quadratic (hatched light yellow) polynomial fits. Note that: a) the five-point quadratic model is consistent with the full cubic model and has a comparable extrapolation error, and b) the inflection point near  $k_F r_e \approx 0.16$  necessitates a higher-order fit for larger ranges (cubic is sufficient for the ranges shown here). Results for  $N_+ = 40$  show the same qualitative behaviour; hence, for the other points we use the five-point quadratic extrapolation.

fixed nodal structure as defined by an initial many-body wave function (ansatz). By varying the ansatz, we obtain a variational upper bound on the ground-state energy. In this work, we use the trial function introduced in [6]:

$$\Psi_T = \mathcal{A}[\phi(\mathbf{r}_{11'})\phi(\mathbf{r}_{22'})\cdots\phi(\mathbf{r}_{nn'})] \prod_{ij'} f(\mathbf{r}_{ij'}), \quad (1)$$

where  $\mathcal{A}$  antisymmetrizes over particles of the same spin (either primed or unprimed) and  $f(\mathbf{r})$  is a nodeless Jastrow function introduced to reduce the statistical error. The antisymmetrized product of  $s$ -wave pairing functions  $\phi(\mathbf{r}_{ij'})$  defines the nodal structure:

$$\phi(\mathbf{r}) = \sum_{\mathbf{n}} \alpha_{\|\mathbf{n}\|} e^{i\mathbf{k}_{\mathbf{n}} \cdot \mathbf{r}} + \tilde{\beta}(\mathbf{r}). \quad (2)$$

The sum is truncated (we include ten coefficients) and the omitted short-range tail is modelled by the phenomenological function  $\tilde{\beta}(\mathbf{r})$  chosen to ensure smooth behavior near zero separation. We use the same form for  $\tilde{\beta}(\mathbf{r})$  as in [6] with the values  $b = 0.5$  and  $c = 5$ , and vary the 10 coefficients  $\alpha_{\|\mathbf{n}\|}$  for each  $N_+$  to minimize the energy as described in Ref. [24]. Representative nodal

$N_+$	$\xi(N_+)$	$\xi_{\text{box}}(N_+)$	$\xi_N/\xi_{\text{box}}$
4	0.280(2)	0.205(1)	1.3641
6	0.380(2)	0.274(1)	1.3880
8	0.400(2)	0.310(1)	1.2890
10	0.405(2)	0.342(1)	1.1849
12	0.405(3)	0.370(2)	1.0930
14	0.400(2)	0.394(2)	1.0145
16	0.397(2)	0.367(2)	1.0827
18	0.394(2)	0.355(1)	1.1122
20	0.392(2)	0.350(2)	1.1197
22	0.387(2)	0.348(2)	1.1144
24	0.388(2)	0.352(2)	1.1017
30	0.382(2)	0.366(2)	1.0444
40	0.381(1)	0.393(1)	0.9699
50	0.380(1)	0.391(1)	0.9726
60	0.381(2)	0.386(2)	0.9869
66	0.382(2)	0.383(2)	0.9950
70	0.386(3)	0.379(3)	1.0177
80	0.385(2)	0.368(2)	1.0461
90	0.384(1)	0.365(1)	1.0498
100	0.385(2)	0.370(2)	1.0403
110	0.382(2)	0.373(2)	1.0236
120	0.379(2)	0.373(2)	1.0173
130	0.380(2)	0.375(2)	1.0139

**Table I.** Values of  $\xi(N_+) = E(N_+)/V/E_{\text{FG}}$  shown in Fig. 1. To facilitate comparison with other normalizations in the literature, we include the values  $\xi_{\text{box}}(N_+) = E(N_+)/E_{\text{FG}}(N_+)$  where  $E_{\text{FG}}(N_+)$  is the energy of  $N_+$  non-interacting particles in a box. The conversion factor is shown in the last column.

structures are defined by the coefficients in Table II. The same ansatz suffices for different effective ranges, but an independent optimization is required for each  $N_+$ .

We simulate the Hamiltonian:

$$\mathcal{H} = \frac{\hbar^2}{2m} \left( - \sum_{\mathbf{k}=1}^{N_+} \nabla_{\mathbf{k}}^2 - 4v_0\mu^2 \sum_{i,j'} \text{sech}^2(\mu r_{ij'}) \right), \quad (3)$$

with an interspecies interaction of the modified Pöschl-Teller type (off-resonance intraspecies interactions are neglected). We tune to infinite  $s$ -wave scattering length by setting  $v_0 = 1$ : the effective range becomes  $r_e = 2/\mu$ . To extrapolate to the zero-range limit, we simulate at  $\mu/k_F \in \{12.5, 24, 36, 48, 60\}$  for which  $0.03 < k_F r_e < 0.16$ . A careful examination of additional ranges up to  $k_F r_e \sim 0.35$  for  $N_+ = 40$  and  $N_+ = 66$  (see the inset in Fig. 1)

$N_+$	$a_0$	$a_1$	$a_2$	$a_3$	$a_4$	$a_5$	$a_6$	$a_8$	$a_9$	$a_{10}$
10	1600	350	49	16	12	14	14	11	9.0	6.7
40	160	91	27	0.49	-2.8	-0.086	2.2	2.9	2.5	1.9
80	-24	13	12	8.2	5.1	3.7	2.7	2.0	1.6	1.0
120	-51	-17	0.51	7.8	6.3	5.8	4.6	2.5	1.7	1.0

**Table II.** Sample coefficients of the pairing function (2)  $\alpha_{\|\mathbf{n}\|} = 10^{-4} a_I$  where  $I = \|\mathbf{n}\|^2 = n_x^2 + n_y^2 + n_z^2 = k^2 L^2 / 4\pi^2$ . Higher-order coefficients are set to zero.

reveals that a three-parameter quadratic model in  $r_e$  is necessary and sufficient to extrapolate our results without a systematic bias; the results are shown in Fig. 1.

The energies exhibit definite finite-size effects for  $N_+ \lesssim 50$ , but are essentially featureless for larger  $N_+$ . This lack of structure is confirmed by the best fit DFT (discussed below) and disagrees with the results presented in Ref. [10]. The values of  $\xi$  for  $N_+ > 50$  are distributed about the best fit value  $\xi_S \approx 0.383(1)$ , and represent the lowest variational bounds to date. Part of the decrease from previous results is due to the careful extrapolation to zero effective range. The remainder is due to the improved optimization of the variational wave function.

To model the finite-size effects we turn to a local DFT for the unitary Fermi gas that generalizes the SLDA originally presented in Ref. [20]. In addition to the total density  $n_+ = 2 \sum_n |v_n|^2$ , the SLDA includes both kinetic  $\tau_+ = 2 \sum_n |\nabla v_n|^2$  and anomalous densities  $v = \sum_n u_n v_n^*$ . (The + index signifies the sum of the contributions coming from the two components a and b;  $u_n(\mathbf{r})$  and  $v_n(\mathbf{r})$  are the Bogoliubov quasiparticle wave functions.) The original three-parameter SLDA is

$$\mathcal{E}_{\text{SLDA}} = \frac{\hbar^2}{m} \left( \frac{\alpha}{2} \tau_+ + \beta \frac{3}{10} (3\pi^2)^{2/3} n_+^{5/3} \right) + g v^\dagger v, \quad (4)$$

where  $\alpha$  is the inverse effective mass;  $\beta$  is the self-energy; and  $\gamma$  controls the pairing through the regularized coupling  $g = 1/(n_+^{1/3}/\gamma - \Lambda/\alpha)$  where  $\Lambda \rightarrow \infty$  is a momentum cutoff that we take to infinity (see Ref. [5] for details). One can use numerically the equations for homogeneous matter in the thermodynamic to replace the parameters  $\beta$  and  $\gamma$  with the more physically relevant quantities  $\xi_S$  and  $\eta = \Delta/E_F$ , where  $\Delta$  is the pairing gap.

In principle, the DFT can be expressed in terms of only the density  $n_+$  and its gradients. References [21] consider local formulations of this type (called Extended Thomas-Fermi (ETF) functionals). Since gradients vanish in the periodic box, ETF functionals reduce to  $\mathcal{E}_{\text{ETF}}(n_+) \equiv \xi_S \mathcal{E}_{\text{FG}}$  and exhibit no finite-size structure, contrary to the QMC results. Reference [19] adds  $\alpha \tau_+$ , but without  $v^\dagger v$  the finite-size effects do not correlate with the QMC behavior (see Fig. 1) and the best fit to our results is also flat ( $\alpha \rightarrow 0$ ). Furthermore, such functionals cannot qualitatively reproduce the quasiparticle dispersion relationship, an attractive feature of the SLDA (see also Ref. [25]).

The best fit three-parameter SLDA functional (4) –  $\alpha = 1.26(2)$ ,  $\xi_S = 0.3826(5)$ , and  $\eta = 0.87(2)$  – is shown in Fig. 1. It fits the 23 QMC points from  $N_+ = 4$  to  $N_+ = 130$  with a reduced chi squared  $\chi_r^2 = 0.7$ , indicating complete consistency. Although remarkable, the fit is not completely satisfactory: 1) Fitting the exact two-particle energy  $\xi_2 = -0.4153 \dots$  raises  $\chi_r^2 = 2.0$ , and 2) the best fit gap parameter  $\eta$  and inverse effective

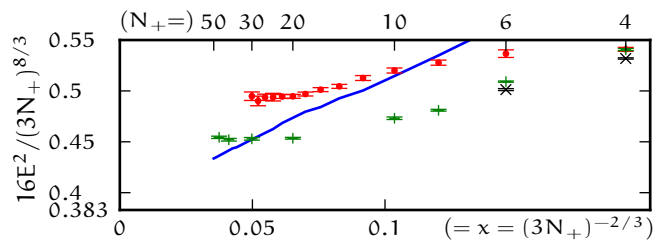


**Figure 2.** (color online) Ground-state energy of the harmonically trapped unitary Fermi gas (in units where  $\hbar\omega = 1$ ) scaled to demonstrate the asymptotic form  $16E^2/(3N_+)^{8/3} = \xi_S(1 + cx + O(x^{7/6}))^2$  predicted by the low-energy effective theory of Ref. [32]. The best fit SLDA (solid blue line) is compared with zero-range results for  $N_+ \in \{4, 6\}$  from Ref. [33], and finite-range QMC results from Ref. [23] (upper red dots) and Ref. [34] (green pluses). The latter have significantly lower energy, despite having a slightly large effective range, suggesting that the wave functions in Ref. [23] were not fully optimized. We expect careful optimization and zero-range extrapolation to bring the QMC results for large  $N_+$  in line with the DFT as discussed in the text.

mass  $\alpha$  are inconsistent with the values  $\eta = 0.50(5)$  and  $\alpha = 1.09(2)$  obtained from the  $N_+ = 66$  QMC quasiparticle dispersion relation [8, 26], and the values  $\eta = 0.45(5)$  [27] and  $\eta = 0.44(3)$  [28] extracted from experimental data.

These deficiencies might be remedied by generalizing the SLDA. As noted in Ref. [5], the following combination of divergent kinetic and anomalous densities is finite:

$$K = \frac{\hbar^2 \tau_+}{2m} + \frac{g}{\alpha} v^\dagger v = \frac{\hbar^2 \tau_+}{2m} + \frac{v^\dagger v}{\alpha n_+^{1/3}/\gamma - \Lambda}. \quad (5)$$

The lack of scales thus dictates the functional form:

$$\mathcal{E}(K, n_+) = \xi(Q) \mathcal{E}_{\text{FG}}(n_+), \quad Q = K/\mathcal{E}_{\text{FG}}(n_+), \quad (6)$$

where  $Q$  is dimensionless, and the regularization condition depends on  $Q$  through the function  $\gamma(Q)$ . The original SLDA is linear  $\xi(Q) = \alpha Q + \beta$  with constant  $\gamma(Q) = \gamma$ . This generalized functional can fit any monotonic  $\xi(N_+)$ , including the exact  $N_+ = 2$  point. For  $N_+ > 6$ ,  $\xi(N_+)$  is not monotonic and the functional is in principle constrained. For example, requiring that  $\xi = \xi_S$  at both  $N_+ \approx 6.2(2)$  and  $N_+ = \infty$  fixes the ratio  $\eta/\alpha = 0.69(2)$ . (As an aside, we note that the momentum distribution  $n_k$  in the DFT relates this to the “contact”  $C$ :  $\eta/\alpha = \sqrt{2C}/k_F^2 \approx 0.44 - 0.49$ ; see Refs. [29] and references therein, though it is not clear that this property should be trusted.) In practice, the errors and the discreteness in  $N_+$  leave room for flexibility in the functional form, and we have found several generalized functional forms with  $\chi_r^2 \approx 1.5$  while constraining  $\eta = 0.50$ . We may have to accept the discrepancy in  $\alpha$  as a limitation of the DFT.

However, generalizing the SLDA may not be needed: analyzing the “symmetric heavy-light ansatz” [30], (justified by lattice QMC calculations [12]), we find that the

simple three-parameter SLDA suffices ( $\chi_r^2 \approx 0.5$ ) with reasonable  $\alpha = 0.96(2)$ ,  $\eta = 0.51(1)$ , and  $\xi = 0.322(2)$  – slightly higher than the  $\xi = 0.31(1)$  extracted in [30].

It is not trivial that the simple DFT (4) captures all finite-size effects above  $N_+ = 4$  to high precision in both calculations, indicating that the SLDA may be used to extrapolate to the thermodynamic limit. We note that no particle-number projection is required – a quite ill-defined procedure often considered necessary in nuclear physics [31]: Perhaps improved nuclear functionals may similarly capture finite-size effects through local anomalous densities in the spirit of  $\nu$ .

To finish, we consider harmonically trapped systems in Fig. 2. As discussed in [32], the energy may be expressed as  $E(N_+) = \frac{1}{2} \hbar \omega \sqrt{\xi_S} (3N_+)^{4/3} (1 + cx + O(x^{7/6}))$  where  $x = (3N_+)^{-2/3}$  and  $c$  is expressed in terms of low-energy coefficients. As demonstrated by the zero-range  $N_+ \in \{4, 6\}$  results of [33], the DFT still over-estimates the energy for small systems, most likely because we have omitted the gradient terms in the functional that vanish in homogeneous systems.

For large  $N_+$  the DFT has the expected asymptotic form with intercept  $\xi_S = 0.383$  unlike the finite-range QMC results of Refs. [23, 34]. This is qualitatively consistent with the leading effective-range corrections which scale asymptotically as  $x^{-1/4}$ ; the systematic overestimation of the energy by the variational QMC approach might also contribute. We defer further discussion until carefully extrapolated zero-range results are published.

To summarize, we present the most precise Quantum Monte Carlo calculations to date of a symmetric unitary Fermi gas in a periodic box comprising 4 to 130 particles. By carefully characterizing and extrapolating these results to zero effective range, we have completely mapped out the finite-size effects. These results are used to analyze the structure of a Density Functional Theory for the symmetric unitary gas, and it is shown that the simplest three-parameter form of Eq. (4) fully accounts for all shell effects to within the statistical errors of the QMC results without the need for particle-number projection; a more complicated form, however, may be required to capture both the finite-size effects and the quasiparticle dispersions. The DFT predicts no significant shell corrections beyond 50 particles, and the QMC calculations confirm this, allowing us to extract a precise upper bound on the universal equation of state  $\xi_S \leq 0.383(1)$ , an order of magnitude improvement in precision over previous bounds and the lowest bound of any variational method to date. The functional in its latest form is well constrained, but leads to slight disagreements with QMC predictions for harmonic traps. Converging both QMC and DFT approaches promises to be a fruitful direction of future research.

We thank Aurel Bulgac, Joe Carlson, and Dean Lee

for useful discussions. This work is supported, in part, by US Department of Energy (DOE) grants DE-FG02-00ER41132, DE-FG02-97ER41014, & DE-AC52-06NA25396, DOE contracts DE-FC02-07ER41457 (UNEDF SCIDAC) & DE-AC52-06NA25396, and by the LDRD program at Los Alamos National Laboratory (LANL). Computations for this work were carried out through Open Supercomputing at LANL, on the UW Athena cluster, and at the National Energy Research Scientific Computing Center (NERSC).

- 
- [1] M. Inguscio, W. Ketterle, and C. Salomon, eds., *Ultra-cold Fermi Gases*, International School of Physics “Enrico Fermi”, Vol. 164 (Ios Press, Amsterdam, 2007); S. Giorgini, L. P. Pitaevskii, and S. Stringari, *Rev. Mod. Phys.* **80**, 1215 (2008).
  - [2] “The Many-Body Challenge Problem (MBX) formulated by G. F. Bertsch in 1999”; G. A. Baker, Jr., *Phys. Rev. C* **60**, 054311 (1999); *Int. J. Mod. Phys. B*, **15**, 1314 (2001).
  - [3] DOE SCIDAC UNEDF project, <http://www.unedf.org/>.
  - [4] A. Gezerlis and J. Carlson, *Phys. Rev. C* **77**, 032801 (2008).
  - [5] A. Bulgac, M. M. Forbes, and P. Magierski in *BCS-BEC Crossover and the Unitary Fermi Gas*, edited by W. Zwerger, Lecture Notes in Physics (Springer, 2011).
  - [6] J. Carlson, S. Y. Chang, V. R. Pandharipande, and K. E. Schmidt, *Phys. Rev. Lett.* **91**, 050401 (2003).
  - [7] G. E. Astrakharchik, J. Boronat, J. Casulleras, and S. Giorgini, *Phys. Rev. Lett.* **93**, 200404 (2004).
  - [8] J. Carlson and S. Reddy, *Phys. Rev. Lett.* **95**, 060401 (2005).
  - [9] A. Gezerlis, S. Gandolfi, K. E. Schmidt, and J. Carlson, *Phys. Rev. Lett.* **103**, 060403 (2009).
  - [10] A. J. Morris, P. López Ríos, and R. J. Needs, *Phys. Rev. A* **81**, 033619 (2010).
  - [11] A. Bulgac, J. E. Drut, and P. Magierski, *Phys. Rev. A* **78**, 023625 (2008).
  - [12] D. Lee, *Phys. Rev. C* **78**, 024001 (2008); T. Abe and R. Seki, *Phys. Rev. C* **79**, 054003 (2009).
  - [13] S. Zhang, K. E. Schmidt, and J. Carlson, private communication; J. Drut, A. Gezerlis, and T. A. Lähde, in preparation (2011); M. Endres, D. Kaplan, J.-W. Lee, and A. Nicholson, in preparation (2011).
  - [14] R. Haussmann, W. Rantner, S. Cerrito, and W. Zwerger, *Phys. Rev. A* **75**, 023610 (2007); Y. Nishida, **75**, 063618 (2007).
  - [15] M. Bartenstein *et al.*, *Phys. Rev. Lett.* **92**, 203201 (2004); J. Kinast *et al.*, *Science* **307**, 1296 (2005); G. B. Partridge, W. Li, R. I. Kamar, Y. an Liao, and R. G. Hulet, **311**, 503 (2006).
  - [16] L. Luo and J. E. Thomas, *J. Low Temp. Phys.* **154**, 1 (2009).
  - [17] N. Navon, S. Nascimbène, F. Chevy, and C. Salomon, *Science* **328**, 729 (2010).
  - [18] J. E. Drut, R. J. Furnstahl, and L. Platter, *Prog. Part. Nucl. Phys.* **64**, 120 (2010); A. Gezerlis and G. F. Bertsch, *Phys. Rev. Lett.* **105**, 212501 (2010); S. Gandolfi, J. Carlson, and S. C. Pieper, *Phys. Rev. Lett.* **106**, 012501 (2011).
  - [19] T. Papenbrock, *Phys. Rev. A* **72**, 041603 (2005).
  - [20] A. Bulgac, *Phys. Rev. A* **76**, 040502 (2007).
  - [21] G. Rupak and T. Schaefer, *Nucl. Phys.* **A816**, 52 (2009);

- L. Salasnich and F. Toigo, Phys. Rev. A **78**, 053626 (2008).
- [22] S. Y. Chang and G. F. Bertsch, Phys. Rev. A **76**, 021603 (2007).
- [23] D. Blume, J. von Stecher, and C. H. Greene, Phys. Rev. Lett. **99**, 233201 (2007).
- [24] S. Sorella, Phys. Rev. B **64**, 024512 (2001).
- [25] A. Bhattacharyya and R. J. Furnstahl, Phys. Lett. B **607**, 259 (2005).
- [26] A. Bulgac and M. M. Forbes, Phys. Rev. Lett. **101**, 215301 (2008).
- [27] J. Carlson and S. Reddy, Phys. Rev. Lett. **100**, 150403 (2008).
- [28] A. Schirotzek, Y. Shin, C. H. Schunck, and W. Ketterle Phys. Rev. Lett. **101**, 140403 (2008).
- [29] S. Gandolfi, K. E. Schmidt, and J. Carlson, Phys. Rev. A **83**, 041601 (2011); J. E. Drut, T. A. Lähde, and T. Ten, arXiv:1012.5474.
- [30] D. Lee, Eur. Phys. J. A **35**, 171 (2008).
- [31] T. Duguet, M. Bender, K. Bennaceur, D. Lacroix, and T. Lesinski, Phys. Rev. C **79**, 044320 (2009).
- [32] D. T. Son and M. B. Wingate, Ann. Phys. (NY) **321**, 197 (2006).
- [33] D. Blume and K. M. Daily, C. R. Phys. **12**, 86 (2011).
- [34] S. Gandolfi, J. Carlson, and K. E. Schmidt, private communication (2010).